The magic number N=28 and the role of the spin-orbit interaction

O. Sorlin

Evolution of the N=28 shell closure far from stability

O. Sorlin

Grand Accélérateur d'Ions Lourds (GANIL), CEA/DSM - CNRS/IN2P3
Bvd Henri Becquerel, BP 55027, F-14076 Caen Cedex 5, France
E-mail: sorlin@ganil.fr

The present contribution focuses on three recent experimental achievements obtained at the GANIL facility on the study of the $N = 28$ shell closure south to the doubly maic nucleus $^{48}_{20}$Ca. First, the single particle energies of the neutron fp states in ^{47}Ar have been determined by transfer (d,p) reaction using a radioactive beam of $^{46}_{18}$Ar$_{28}$. A reduction of the $N = 28$ gap and of the SO splittings of the f and p states is found. Second, an $E0$ isomer has been discovered in $^{44}_{16}$S$_{28}$ which is suggestive of a shape mixing. Third, the energy of the first 2^+ state of $^{42}_{14}$Si$_{28}$ has been obtained through in-beam γ-ray emission induced by a 2 protons knock-out reaction. Its low value, 770(19) keV, points to a large deformation there. The gradual change from spherical to deformation in the $N = 28$ isotones from $Z = 20$ to $Z = 14$ is ascribed to specific proton-neutron interactions and to enhanced quadrupole correlations. A global description of all the physics involved at $N = 28$ is derived along with experimental results.

Keywords: Shell closure, transfer (d,p), spectroscopic factor, single particle energy, isomer E0, in-beam spectroscopy, tensor force, spin-orbit interaction

1. Introduction

The magic number 28, revealed for instance in the doubly magic nucleus $^{48}_{20}$Ca, is the first originating from the spin-orbit (SO) coupling in atomic nuclei. The SO interaction lowers the $f_{7/2}$ neutron orbit just into the middle of the gap between the sd and fp oscillator shells, resulting in a neutron magic number at $N = 28$ between the $f_{7/2}$ and $p_{3/2}$ orbits. The sequence of the neutron orbits around $N = 28$ exhibits 2 pairs of spin-orbit partners $f_{7/2}$, $p_{3/2}$, $p_{1/2}$ and $f_{5/2}$, ranked as a function of decreasing binding energies. The evolution of the $N = 28$ shell gap is therefore potentially linked to changes in the SO splitting. Variation of these neutron orbits south to ^{48}Ca as protons are progressively removed from the quasi-degenerate $s_{1/2}$ and $d_{3/2}$ orbits can be traced back to the nuclear forces V^{pn} involving protons and neutrons in the sd and fp shells, respectively.

In case of a reduction of the $N = 28$ shell gap quadrupole collectivity (E2) is likely to be favored across it, i.e. between the occupied ($f_{7/2}$; $\ell = 3$) and valence states ($p_{1/2}$, $p_{3/2}$; $\ell = 1$) which differ by two units of angular momentum. As this peculiar quadrupole symmetry exists as well for protons in the sd shells, the rigidity of the $^{44}_{16}$S$_{28}$ and $^{42}_{14}$Si$_{28}$ isotones against quadrupole deformation depends on the size

of the spherical proton ($Z = 16, 14$) and neutron $N = 28$ shell gaps.

The present review focuses on recent experimental achievements obtained at the GANIL facility the last few years on the evolution of the $N = 28$ shell closure. Different methods have been used, such as (i) the neutron stripping reaction $^{46}_{18}$Ar(d,p) to determine the neutron single particle energies of the f and p states in $^{47}_{18}$Ar,[1] (ii) the delayed electron spectroscopy to find a shape isomer in $^{44}_{16}$S,[2] (iii) the in-beam γ-ray spectroscopy to determine the energy of the first 2^+ state in $^{42}_{14}$Si.[3] The salient features from these experiments are described in the following paragraphs.

2. Study of the neutron single particle states in ^{47}Ar

A pure ^{46}Ar radioactive beam of 10.2(1) A·MeV was delivered by the SPIRAL facility[4] at a mean intensity of $2{\cdot}10^4$ pps. It was guided with a parallel optics onto a 0.38(6) mg/cm^2 thick CD_2 target in which the ^{46}Ar(d,p)^{47}Ar transfer reaction took place. The position of the beam on the target was obtained event by event with a resolution (FWHM) of 1 mm using a position-sensitive Multi Wire Proportional Chamber (MWPC)[5] placed 11 cm downstream from the target. The energy and angle of the reaction protons were measured with the MUST detector array[6] comprising eight highly segmented double-sided Si detectors covering polar angles ranging from 110 to 170° with respect to the beam direction. The transfer-like products ^{47}Ar(^{46}Ar) were selected and identified by the SPEG[7] spectrometer in the case of a neutron pick-up to bound(unbound) states in ^{47}Ar.

The excitation energy spectrum of Fig. 1(a) was obtained using the proper kinematics relations. It has been fitted using a sum of 9 gaussian curves of width σ=175 keV. The Q value of the transfer reaction to the ground state (GS) of ^{47}Ar is Q=1.327(80) MeV, leading to a mass excess Δm(^{47}Ar)=-25.20(9) MeV. The present mass excess value gives rise to an N=28 gap of 4.47(9) MeV in ^{46}Ar, which is 330(90) keV smaller than in ^{48}Ca.

Experimental proton angular distributions are shown in Fig. 1 for the ground state (top) and for the second excited state (bottom). From a comparison to Distorted Wave Born Approximation (DWBA) calculations using the DWUCK4[8] code and the optical potentials of Ref.,[9,10] the transferred angular momentum ℓ and the vacancy $(2J + 1)C^2S$, [C^2S being the Spectroscopic Factor (SF), J the total spin value] of individual orbitals in ^{47}Ar have been determined. Similar procedure has been applied to all other peaks,[1] which are not shown here. The first two peaks were attributed to $\ell = 1$ transfer to p tates, and the third one to an $\ell = 3$ transfer to the $f_{7/2}$ state. The angular distribution of the three peaks around 3.4 MeV (Fig. 1) was reproduced with a combination of ℓ=3 and ℓ=4 components. The ℓ=3 part is most likely contained in the first two peaks as the ℓ=4 transfer to the $g_{9/2}$ state is located at $\simeq$4 MeV in other N=29 isotones. An ℓ=4 value was unambiguously attributed to the 5500(85) keV state.

For a closed-shell nucleus, the total vacancy is expected to be equal to $2J+1$ for the valence orbitals (such as the GS), and 0 for occupied ones (such as the $f_{7/2}$ orbit).

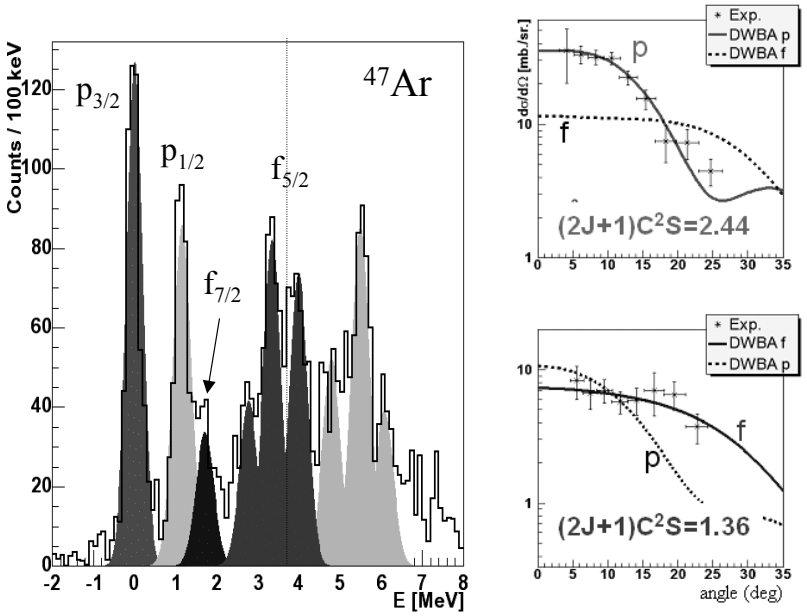

Fig. 1. Left: Background subtracted inclusive spectrum fitted by means of 9 gaussian, Right : Experimental proton angular distributions of the ground state (top) and of the second excited state (bottom) in ^{47}Ar. The curves correspond to DWBA calculations assuming transfer to p and f states are shown for comparison.

The GS vacancy value of ^{47}Ar, (2.44(20)), is significantly smaller than its maximum value of 4. As a matter of comparison, that of ^{49}Ca is 3.36(14) using similar global optical potentials. This means that a fraction of neutrons is already occupying the valence $p_{3/2}$ orbit in the ^{46}Ar nucleus core. It turns out that the missing vacancy value (1.56) of the $p_{3/2}$ GS counterbalances the excess (1.36 instead of 0) of the 1740 keV state, meaning that some of the $f_{7/2}$ neutrons have moved to the $p_{3/2}$ orbital in ^{46}Ar. This confirms that some amount of neutron particle-hole excitation is already occuring across $N = 28$ in ^{46}Ar. This process likely due to the reduction of the $N = 28$ shell gap and to the increase of correlations. It will be reinforced if further reduction of the $N = 28$ shell gap occurs for lower Z values.

The structure of ^{47}Ar was calculated in the Shell Model (SM) framework using the ANTOINE code[11] and the *sdpf* interaction[12] to which the relevant neutron-proton monopole interactions V^{pn} were modified[13] to reproduce the experimental binding energies and spectroscopic factors of the known p states in ^{45,47}Ar[13–15] and ^{47,49}Ca.[16] By applying this constraint, the full particle strength of the $\nu f_{7/2}$, $\nu p_{3/2}$ and $\nu p_{1/2}$ and $\nu f_{5/2}$ orbits has been determined in ^{47}Ar. The resulting Single Particle Energies (SPE) are compared to those of the $^{49}_{20}$Ca isotone[17,18] in Fig. 2. Between the two isotones 2 protons have been removed, leading to a 'natural' decrease of the binding energies of all fp states due to 'missing' proton-neutron interactions. Bearing in mind that the $d_{3/2}$ and $s_{1/2}$ orbitals are quasi-degenerate in ^{48}Ca,[19] the

removal of 2 protons is equiprobable from these orbits. If the nuclear forces between protons and neutrons involved for each orbits were similar in strength this decrease would have been the same for all the f and p states. Rather their binding energy vary differently. The orbits in which the angular momentum is aligned ($\ell_\uparrow$) with the intrinsic spin, such as $f_{7/2}$ and $p_{3/2}$, become relatively much less bound than the $f_{5/2}$ and $p_{1/2}$ orbits where the angular momentum and intrinsic spin are anti-aligned ($\ell_\downarrow$). From these experimental trends, it is found that the proton-neutron monopole matrix elements involving the $d_{3/2}$ and $s_{1/2}$ protons with the neutron fp orbits should contain a spin-dependent term $\tilde{V}$ in addition to the central part of the interaction. Quantitatively, values of $\tilde{V}^{pn}_{d_{3/2}f_{\downarrow,\uparrow}}$ have been determined to be +280 keV (repulsive) and -210 keV (attractive) for the $f_{5/2}$ and $f_{7/2}$ orbitals, respectively. In this case, the change of the f SO splitting was tentitavely attributed to the action of tensor forces between the $d_{3/2}$ protons and the f neutrons.[1,20] The change of the p SO splitting was ascribed to the removal of a certain fraction of $s_{1/2}$ protons, and to a much weaker extent to the removal of $d_{3/2}$ protons. This latter constraint is provided by the fact that the p SO splitting remains constant ($\simeq$1.7 MeV) between ${}^{41}_{20}\mathrm{Ca}_{21}{}^{18}$ and ${}^{37}_{16}\mathrm{S}_{21}{}^{21}$ after the removal of four protons from the $d_{3/2}$ orbit. As the protons $s_{1/2}$ occupy the center of the nucleus, the change of the neutron p SO is due to depletion of central density of the nucleus. This points to the central density dependence of the SO interaction, which was usually thought to be a surface term exclusively. Details on this interaction can be found in Refs.[1,22] For the $p_{1/2}$ and $p_{3/2}$ orbitals, we have extracted $\tilde{V}^{pn}_{s_{1/2}p_{\downarrow,\uparrow}}$ of +170 keV and -85 keV, respectively. With these effects, the spin-orbit splittings for the f and p states have been reduced by about 10%[1,13] between ^{49}Ca and ^{47}Ar, by the removal of only two protons.

The variation of the single particle energies in term of monopole terms can be pursued towards the ${}^{43}_{14}$Si nucleus in which, as compared to ${}^{49}_{20}$Ca, 4 protons have been removed from the $d_{3/2}$ and 2 from the $s_{1/2}$ orbits. Using the monopole matrix elements derived in the interaction, a global shrink between the fp orbits is foreseen, such as reductions of the (i) $N = 28$ gap by $330 \times 3 \simeq 1000$ keV, (ii) f SO splitting by $4(0.28 + 0.21) \simeq 2000$ keV and (iii) p SO splittiing by $2(0.17 + 0.085) \simeq 500$ keV. This global shrink of SPE is expected to reinforce particle-hole excitations across $N = 28$, which are of quadrupole nature. Consequently a progressive increase of collectivity, or onset of quadrupole deformation would develop below $Z = 18$. A search for a shape coexistence or mixing between a spherical and deformed state was searched for in ${}^{44}_{16}\mathrm{S}_{28}$ to ascertain the hypothesis discussed above.

3. Electron spectroscopy of ^{44}S

In ${}^{44}_{16}\mathrm{S}_{28}$ the 2^+_1 energy and the $B(E2)$ value were found to be intermediate between a deformed and a spherical nucleus.[23] This situation is suggestive of a possible shape mixing between two configurations, an assumption which can be confirmed by the search for a low lying 0^+_2 state. A secondary beam of ^{44}S was produced by the fragmentation of a ^{48}Ca beam at 60A·MeV into a Be target, and selected by the

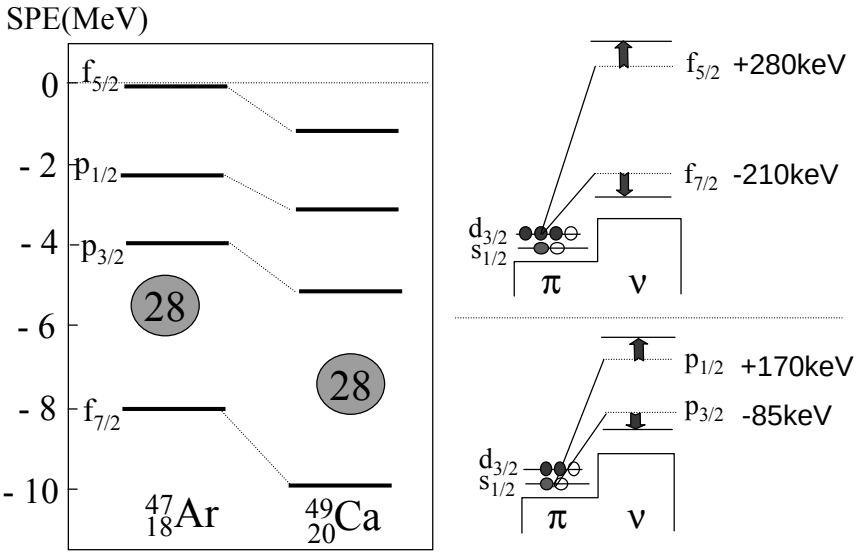

Fig. 2. Left : Neutron single particle energies (SPE) of the fp orbitals for the $^{47}_{18}Ar_{29}$ and $^{49}_{20}Ca_{29}$ nuclei. Right : Schematic view of the proton-neutron interactions invloved to change the f (top) and p (bottom) SO splittings.

LISE achromatic spectrometer. During this reaction mechanism part of the nuclei can be produced in a 0^+_2 state, which can be isomer or not. To search for an isomer transition, these nuclei were implanted in a thin mylar foil located at the center of an array of four Si-Li and two Ge cristals detectors which aimed at detecting conversion electrons and γ-rays, respectively. Such a 0^+_2 state was discovered through the detection of a delayed electron transition at an energy of 1362.5(1)keV[2] with a lifetime of $2.3 \pm 0.5\ \mu s$. Combining the conversion-electron and γ-ray spectroscopy it was found that the 0^+_2 state decays both directly to the ground state via internal conversion, and to the 2^+_1 state at 1329 keV. This experiment has been repeated few months ago to obtain more statistics and to be able to determine the ratio between the two reduced transition probabilities, B(E2;$0^+_1 \rightarrow 2^+_1$) [obtained in Ref.[23]] and B(E2;$0^+_2 \rightarrow 2^+_1$) [determined in the present experiment]. The analysis is in progress. Similar and large B(E2) values would reveal that the 0^+_1 and 0^+_2 levels have mixed wave functions. A large reduced strength $\rho(E0)$ would in turn point to the existence of a spherical and strongly deformed configurations in ^{44}S which co-exist before mixing.

4. Determination of the 2^+ energy in ^{42}Si

Excited states in the neutron-rich $_{14}$Si isotopes have been recently discovered at the NSCL [24] and GANIL laboratories.[3] These two experiments used nucleon removal reactions from secondary beams centered around ^{42}P and ^{44}S at intermediate energy

to produce the ^{40}Si and ^{42}Si nuclei and study the γ-rays from their de-excitation in flight. The detection of the γ-rays was achieved by arrays of detectors which surrounded the production target in which the reaction occurred. In the case of Ref.[24] a segmented array of Ge detectors was used, leading to a photo-peak γ-ray efficiency of about 3% at 1 MeV. An array composed of 70 BaF_2 detectors was used in Ref.[3] in order to obtain a higher photo-peak efficiency of about 30% at 1 MeV and 20% at 2 MeV. Campbell et al.[24] have determined the energy of the 2^+ state in $^{40}_{14}Si_{26}$ at 986(5) keV. While the 2^+ energies increase in Ca isotopes from $N = 24$ to reach a maximum around 4 MeV at $N = 28$, the 2^+ energies in the Si isotopes start to deviate from those of the Ca isotopes at $N = 26$ (see Fig. 3) which hints for a reduced N=28 shell gap.[24] As 2^+ neutron excitations occurring before the complete filling of the $\nu f_{7/2}$ shell can be generated inside the shell, they are not that sensitive to the size of the $N = 28$ gap. Conversely, in $^{42}_{14}Si_{28}$ the neutron $f_{7/2}$ shell is *a priori* filled, and the 2^+ state comes mainly from particle-hole excitations across the $N = 28$ gap. It is therefore extremely sensitive to any reduction of the $N = 28$ shell gap. Bastin et al.[3] have established a 2^+ at 770(19) keV for the $N = 28$ nucleus ^{42}Si.

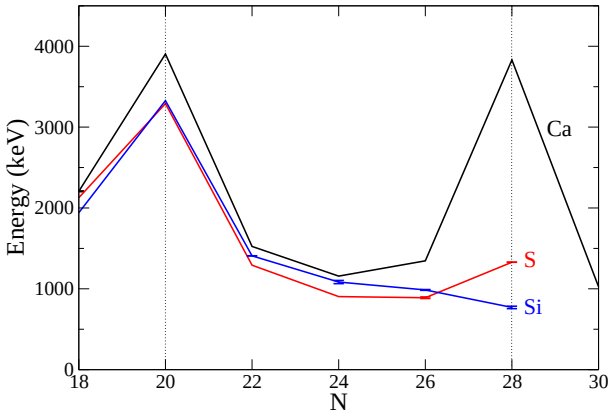

Fig. 3. Experimental E(2_1^+) values in the $_{14}$Si, $_{16}$S and $_{20}$Ca isotopic chains as a function of the neutron number N. Data are taken from the compilation of Ref.,[25] except for ^{38}Si,[26] ^{40}Si,[24] ^{42}Si,[3] and ^{40}S.[27]

As shown in Fig. 3 this dramatic decrease of 2^+ energy ^{42}Si is a proof of the disappearance of the spherical $N = 28$ shell closure at $Z = 14$. This extremely low energy of 770 keV -actually one of the smallest among nuclei having a similar atomic mass - cannot be obtained solely from neutron excitations. Proton core excitations should play an important role, which could in principle be evidenced by measuring the B(E2) values in the Si isotopic chain while reaching $N = 28$.

The behaviors of the $N = 20$ to $N = 28$ isotones south of Ca isotopes are significantly different and instructive. The $N = 20$ shell gap persists with up to the removal of 4 and 6 protons to reach the quasi doubly magic $^{36}_{16}S_{20}$ and $^{34}_{14}Si_{20}$ nuclei, respectively. For these nuclei the existence of significant proton sub-shell closures at $Z = 16$ and $Z = 14$ and the persistence of the $N = 20$ gap are warrants of their rigidity against quadrupole excitations. Conversely, at $N = 28$ the studies of the proton[19] and neutron single particle energies [1,17,18] have revealed a much different situation. The combined compression of the energy of the proton and neutron orbits, plus the favored quadrupole excitations across $N = 28$, produce a rich variety of behaviors and shapes in the even $N = 28$ isotones; spherical ^{48}Ca; oblate non-collective ^{46}Ar; coexistence in ^{44}S, and rotor oblate ^{42}Si .[3,28] This variety of shapes is also supported by mean field calculations, relativistic[29] or non-relativistic.[30–33] In these models subtle changes in the potential energy surfaces arise from the choice of the effective interactions, in particular for the ^{44}S nucleus. However the global trend to deformation is found as the quadrupole symmetry between the occupied and valence protons and neutrons orbits dominates over effects of the residual proton-neutron interaction.

5. Summary

The spectroscopy of the neutron-rich $N = 28$ isotones has been investigated at GANIL by various complementary methods, such as the neutron stripping (d,p), electron spectroscopy, and in-beam γ-ray spectroscopy. By gathering all pieces of information, a coherent description of the evolution of the $N = 28$ shell gap with the physics processes involved has been proposed.

The $N = 28$ shell gap, as well as the neutron f and p SO splittings are significantly reduced. Reasons for this were attributed to a subtle combination of tensor, central and SO forces. This global shrink of SPE favors the developpement of quadrupole deformation south to ^{48}Ca. These reductions of SO splittings arise from new effects that have been put forward these last few years both from theoretical and experimental point of views. In intensity these reduction of SO splittings are much larger than the ones expected by an increased diffuseness of the nuclear matter far from the valley of stability. They are opening up a new vista on the various components giving rise to changes of the SO splittings in hitherto unknown parts of the chart of nuclides. Noteworthy is the fact that similar physics processes (tensor force and $E2$ symmetry) are expected to be at play in other doubly magic nuclei formed by the SO interaction, such as $^{78}_{50}Ni_{28}$ and $^{100}_{50}Sn_{50}$.

6. Acknowledgements

I wish to thank all my collegues (physicists and technicians) who have participated in the mounting, analysis and theoretical interpretation of the experiments presented in this review. Special thanks are addressed to the students, post-docs and

researchers, L. Gaudefroy, S. Grévy B. Bastin, D. Sohler and I. Stefan who have been taking a decisive part in particular for the data analysis. The MUST collaboration have played a key role for the success of the (d,p) experiment, thank's to the diverse and complementay comptences from the IPN Orsay, SPhN Saclay and GANIL laboratories. I have appreciated and learnt very much from efficient collaborations with F. Nowacki, A. Poves, T. Otsuka and J. Pieckarewicz. I also thank few other collaborators who keep on bringing efforts and ideas on the subject, F. Azaiez, Z. Dombràdi, D. Guillemaud-Mueller, K. L. Kratz, M. G. Saint-Laurent and M. Stanoiu.

References

1. L. Gaudefroy et al, Phys. Rev. Lett. **97**, 092501 (2006)
2. S. Grévy et al, Eur. Phys. J. A **25**, s01-111 (2005)
3. B. Bastin et al., Phys. Rev. Lett. **99**, 022503 (2007)
4. A.C.C. Villari *et al.*, Nucl. Instr. Meth. B **204**, 173 (2003)
5. S. Ottini-Hustache *et al.*, Nucl. Instr. Meth. A **431**, 476 (1999)
6. Y. Blumenfeld *et al.*, Nucl. Instr. Meth. A **421**, 471 (1999)
7. L. Bianchi *et al.*, Nucl. Instr. Meth. A **276**, 509 (1989)
8. P. D. Kunz, University of Colorado, (unpublished)
9. G. L. Wales and R. C. Johnson, Nucl. Phys. A **274**, 168 (1976)
10. R. L. Varner *et al.*, Phys. Rep. **201**, 57 (1991)
11. E. Caurier, ANTOINE code, IReS, Strasbourg 1989-2002; E. Caurier and F. Nowacki, Act. Phys. Pol. B **30**, 705 (1999)
12. S. Nummela *et al.*, Phys. Rev. C **63**, 044316 (2001)
13. L. Gaudefroy et al, Phys. Rev. Lett. **99**, 099202 (2007)
14. L. Gaudefroy *et al.*, Eur. Phys. J. A **27** s01, 309 (2006)
15. A. Gade *et al.*, Phys. Rev. C **71**, 051301(R) (2005)
16. ENSDF database, http://www.nndc.bnl.gov/ensdf/
17. R. Abegg *et al.*, Nucl. Phys. A **303**, 121 (1978)
18. Y. Uozumi *et al.* Nucl. Phys. A **576**, 123 (1994)
19. P. D. Cottle *et al*, Phys. Rev. C **58**, 3761 (1998)
20. T. Otsuka *et al.*, Phys. Rev. Lett. **95**, 232502 (2005)
21. C. E. Thorn *et al.*, Phys. Rev. C **30**, 1442 (1984)
22. B. G. Todd-Rutel *et al.*, Phys. Rev. C **69**, 021301(R) (2004)
23. T. Glasmacher *et al*, Phys. Lett. B **395**, 163 (1997)
24. C.M. Campbell *et al.*, Phys. Rev. Lett. **97**, 112501 (2006)
25. S. Raman, C.W. Nestor, and P. Tikkanen, At. Data Nucl. Data Tables **78**,1 (2001)
26. X. Liang *et al.*, Phys. Rev. C. **67**, 024302 (2003)
27. J.A. Winger *et al.*, Phys. Rev. C. **64**, 064318 (2001)
28. E. Caurier F. Nowacki and A. Poves *Nucl. Phys.* A742, 14 (2004)
29. G.A. Lalazissis *et al.*,Phys. Rev. C **60**, 014310 (1999)
30. T.R. Werner *et al.*, Nucl. Phys. A **597**, 327 (1996)
31. P.-G. Reinhardt *et al.*, Phys. Rev. C **60**, 014316(1999)
32. S. Péru *et al.*, Eur. Phys. J. A **49**, 35 (2000)
33. R. Rodriguez-Guzman *et al.*, Phys. Rev. C **65**, 024304 (2002)